

# Cooperation of the proapoptotic receptor agonist rhApo2L/TRAIL with the CD20 antibody rituximab against non-Hodgkin lymphoma xenografts

Dylan Daniel,<sup>1</sup> Becky Yang,<sup>1</sup> David A. Lawrence,<sup>1</sup> Klara Totpal,<sup>2</sup> Inessa Balter,<sup>2</sup> Wyne P. Lee,<sup>3</sup> Alvin Gogineni,<sup>4</sup> Mary J. Cole,<sup>4</sup> Sharon Fong Yee,<sup>2</sup> Sarajane Ross,<sup>2</sup> and Avi Ashkenazi<sup>1</sup>

<sup>1</sup>Departments of Molecular Oncology, <sup>2</sup>Translational Oncology, <sup>3</sup>Immunology, and <sup>4</sup>Biomedical Imaging Group, Genentech, South San Francisco, CA

**Recombinant human rhApo2L/TRAIL selectively stimulates apoptosis in various cancer cells through its receptors DR4 and DR5, and is currently in clinical trials. Preclinical studies have established antitumor activity of rhApo2L/TRAIL in models of epithelial cancers; however, efficacy in non-Hodgkin lymphoma (NHL) models is not well studied. Of 7 NHL cell lines tested in vitro, rhApo2L/TRAIL stimulated apoptosis in BJAB, Ramos RA1, and DoHH-2 cells. Rituximab, a CD20 antibody used to treat certain types of NHL, augmented**

**rhApo2L/TRAIL-induced caspase activation in Ramos RA1 and DoHH2 but not BJAB or SC-1 cells, through modulation of intrinsic rather than extrinsic apoptosis signaling. In vivo, rhApo2L/TRAIL and rituximab cooperated to attenuate or reverse growth of tumor xenografts of all 4 of these cell lines. Depletion of natural killer (NK) cells or serum complement substantially reduced combined efficacy against Ramos RA1 tumors, suggesting involvement of antibody-dependent cell- and complement-mediated cytotoxicity. Both agents exhibited greater activity against disseminated than subcuta-**

**neous BJAB xenografts, and worked together to inhibit or abolish disseminated tumors and increase survival. Moreover, rhApo2L/TRAIL helped circumvent acquired rituximab resistance of a Ramos variant. These findings provide a strong rationale for clinical investigation of rhApo2L/TRAIL in combination with rituximab as a novel strategy for NHL therapy. (Blood. 2007;110:4037-4046)**

© 2007 by The American Society of Hematology

## Introduction

Effective treatments for non-Hodgkin lymphoma (NHL) remain a serious unmet medical need: The incidence of NHL continues to rise,<sup>1</sup> and NHL tumors can relapse in patients who initially respond to treatment. NHL represents a collection of more than a dozen different cancers of lymphocytes. The most prevalent forms of NHL are B-cell malignancies, of which follicular lymphoma (FL) and diffuse large B-cell lymphoma (DLBCL) comprise the majority.<sup>2</sup> Burkitt lymphoma is a less prevalent form of NHL characterized by translocation of the c-myc oncogene to the Ig heavy chain promoter/enhancer region.<sup>3</sup> The monoclonal anti-CD20 antibody rituximab is currently used in the clinic for the treatment of both FL<sup>4-7</sup> and DLBCL.<sup>8</sup> Expression of the CD20 antigen is restricted to B cells; however, the biologic function of CD20 is not fully understood.<sup>9,10</sup> Studies in mice suggest that Fc-mediated effector functions, including antibody-dependent cell-mediated cytotoxicity (ADCC) and complement-dependent cytotoxicity (CDC), are important for the antitumor efficacy of rituximab in vivo.<sup>11,12</sup> A valine (V) polymorphism at amino acid 158 in Fc gamma receptor IIIa (Fc gamma RIIIa) confers higher affinity to human IgG1 than the phenylalanine (F) allele, and effector cells bearing the V allele mediate ADCC more effectively.<sup>13,14</sup> NHL patients homozygous for the V polymorphism in Fc gamma RIIIa show a better response to rituximab, supporting the importance of ADCC for rituximab activity.<sup>15,16</sup> Rituximab has been reported to promote apoptosis in some NHL cell lines in vitro without requirement for ADCC or CDC.<sup>17</sup> Furthermore, there is evidence that rituximab can

sensitize NHL cells to apoptosis by chemotherapeutic drugs in vitro.<sup>18,19</sup>

Apo2 ligand/tumor necrosis factor–related apoptosis-inducing ligand (Apo2L/TRAIL) stimulates apoptosis in various cancer cell types by acting through its cognate proapoptotic receptors DR4 and/or DR5 and stimulating the extrinsic pathway.<sup>20,21</sup> Upon binding to DR4 and/or DR5 at the cell surface, Apo2L/TRAIL induces recruitment of the cytoplasmic adaptor protein FADD (Fas-associated death domain)<sup>22,23</sup> to the intracellular portion of DR4 and DR5. FADD recruits the apical apoptosis-initiating proteases caspases-8<sup>22,23</sup> and -10,<sup>24-26</sup> completing formation of the death-inducing signaling complex (DISC).<sup>27</sup> DISC association leads to activation and self-processing of the apical caspases, releasing active caspase molecules into the cytoplasm, where they cleave and activate downstream effector caspases such as caspases-3, -6, and -7, which execute the apoptosis program. In “type I” cells, stimulation of the extrinsic pathway is sufficient for commitment to apoptotic death. In “type II” cells, this commitment requires further signal amplification through the “intrinsic” pathway.<sup>28,29</sup> This latter amplification occurs through caspase-8–mediated cleavage of the Bcl-2 homology domain 3 (BH3) protein Bid.<sup>30</sup> In turn, truncated Bid binds antiapoptotic Bcl-2 family members such as Bcl-2, Bcl-x<sub>L</sub>, Bcl-w, and A1.<sup>31,32</sup> This frees the proapoptotic Bcl-2 family members Bax and Bak to engage the mitochondria and induce the release of mitochondrial cytochrome *c* and Smac/Diablo into the cytosol, where these latter factors promote caspase activation. Cytochrome *c* forms the “apoptosome” complex with the adaptor

Submitted February 27, 2007; accepted August 17, 2007. Prepublished online as *Blood* First Edition paper, August 27, 2007; DOI 10.1182/blood-2007-02-076075.

The online version of this article contains a data supplement.

The publication costs of this article were defrayed in part by page charge payment. Therefore, and solely to indicate this fact, this article is hereby marked “advertisement” in accordance with 18 USC section 1734.

© 2007 by The American Society of Hematology

Apaf-1 and activates the apoptosis-initiating protease caspase-9, which then stimulates effector caspases. Smac/Diablo binds to inhibitor of apoptosis proteins (IAPs), preventing their negative-regulatory binding to caspases-9 and -3 and hence augmenting apoptosis induction.<sup>33</sup>

There is evidence from mouse models that Apo2L/TRAIL is involved in immunity against certain pathogens as well as in antitumor immune surveillance.<sup>34-36</sup> The full-length ligand is a type 2 cell surface protein, but it also can be shed from T cells through proteolytic processing to form a soluble protein.<sup>37</sup> We have generated an optimized, nontagged soluble recombinant human (rh) Apo2L/TRAIL based on the protein's extracellular region.<sup>38</sup> Crystallographic and biochemical studies reveal that Apo2L/TRAIL is a homotrimeric protein containing an internal zinc molecule that is coordinated by 3 cysteines, located at amino acid position 230 of each subunit.<sup>39-41</sup> Zinc coordination is important for the stability of rhApo2L/TRAIL as a soluble homotrimeric molecule; indeed, it is the zinc-bound form of the ligand that displays optimal selectivity for cancer cells over normal cells, including hepatocytes.<sup>42-45</sup>

Several studies in mice demonstrate that rhApo2L/TRAIL can exert apoptosis-based antitumor activity against human tumor xenografts of several epithelial malignancies including colon, non-small cell lung and pancreatic cancer, as well as in models of nonepithelial cancers such as glioblastoma and multiple myeloma.<sup>21,46,47</sup> However, to our knowledge, there are no published reports on rhApo2L/TRAIL activity against NHL xenografts. In the present study, we examined the proapoptotic activity of rhApo2L/TRAIL against a number of NHL cell lines, as well as the ability of this ligand to cooperate with rituximab. Our results suggest that an approach that integrates the proapoptotic activity of rhApo2L/TRAIL with antibody-mediated effector functions of rituximab should be considered for investigation in NHL patients.

## Materials and methods

### Reagents and cell lines

The BJAB, Ramos RA1, SC-1, Raji, Daudi, and 293 cell lines were obtained from the American Type Culture Collection (Manassas, VA). The DoHH-2, OCI-Ly19, and Colo678 cell lines were obtained from the German Collection of Microorganisms and Cell Cultures (Braunschweig, Germany). Ramos T1 was generated at Genentech (South San Francisco, CA) by inoculation of Ramos RA1 cells into CB 17 ICR severe combined immunodeficient (SCID) mice and allowed to grow to 200 mm<sup>3</sup>. The mice were treated with 500 mg rituximab (20 mg/kg) intraperitoneally 3 times per week for 3 weeks. The resistant tumors that grew out were similar in size to control-treated tumors and were re-established in tissue culture. This clone was found to be refractory to 10 mg/kg rituximab treatment as a xenograft. rhApo2L/TRAIL was generated at Genentech, and endotoxin levels were determined to be less than 0.06 EU/mg by limulus amoebocyte lysate (LAL) assay (BioWhittaker, Walkersville, MD).

### Generation of BJAB- and Ramos RA1-transfected cell lines

**BJAB-Luc cell line.** The retroviral construct pQCXIH.Luc was generated by cloning the firefly luciferase gene into the pQCXIH retroviral vector (BD Clontech, San Diego, CA). Retroviral production and infection were modified from existing protocols.<sup>48,49</sup> Briefly, Phoenix Amphi packaging cells (Orbigen, San Diego, CA) were transfected with pQCXIH.Luc using calcium phosphate. Viral supernatant was collected from these cultures, supplemented with 10 µg/mL polybrene, and added undiluted to BJAB cells plated into 6-well plates. These plates were then centrifuged at room temperature at 300g for 45 minutes. Cells were placed into a 32°C incubator

for 11 hours to allow viral infection. This procedure was repeated every 12 hours with fresh virus for 2 additional times. Following the third infection, remaining virus was removed and replaced with fresh medium. Cells were then allowed to recover for 48 hours in a 37°C incubator prior to selection with 400 µg/mL hygromycin for 1 week. The pool of transfected cells was screened for stable luciferase expression for 30 days prior to use in subsequent experiments.

**Ramos RA1-hBcl2 cell line.** The coding region of human Bcl-2 was cloned into the pMSCV retroviral vector containing a ZsGreen fluorescence protein marker (BD Clontech). Ramos RA1 cells were infected as described for BJAB-Luc cell line.

### Flow cytometry

The analysis of cell surface molecules on lymphoma cell lines was determined using a phycoerythrin (PE)-conjugated mouse monoclonal antibody to human CD20 (BD Biosciences, San Diego, CA); PE-conjugated mouse monoclonal antibodies to human DR4, DR5, DcR1, and DcR2 (eBioscience, San Diego, CA); and fluorescein isothiocyanate (FITC)- and PE-conjugated mouse monoclonal antibodies to CD55 and CD59, respectively (Caltag, Carlsbad, CA). The analysis of murine natural killer (NK) cell content was determined using a PE-conjugated antibody to CD49b (DX5; BD Biosciences, San Diego, CA). Active caspase-3<sup>50</sup> and Bcl-2 were detected by fixation of the cells with Cytofix/Cytoperm buffer, followed by staining with a FITC-conjugated rabbit anti-active caspase-3 or PE-conjugated monoclonal antibody to human Bcl-2 in permeabilization buffer (buffers and stains from BD Biosciences, San Diego, CA). Mitochondrial membrane polarization was detected using DiIC<sub>1</sub>(5) (Molecular Probes, Eugene, OR). Cells were analyzed on a FACSCalibur machine (BD Biosciences, San Jose, CA).

### Cell viability assay

The cells (20 000 cells/well) were treated with rhApo2L/TRAIL alone, rituximab alone, or with the combination of both, and the plates were incubated for 2 days at 37°C. AlamarBlue (Trek Diagnostic Systems, Cleveland, OH), a fluorometric/colorimetric dye, was used as a growth indicator. Fluorescence was read using 96-well fluorometer with excitation at 530 nm and emission of 590 nm. The results are expressed in relative fluorescence units (RFU). For data analysis, the 4-parameter curve-fitting program Kaleidagraph (Synergy Software, Reading, PA) was used.

### Immunoblots and DISC assays

Cell lysates were prepared in phosphate-buffered saline (PBS) containing 1% Triton X-100, separated on 4% to 20% Tris-Bis polyacrylamide gels, and transferred to nitrocellulose membrane. Nitrocellulose was blocked with 1% bovine serum albumin/PBS, and proteins were detected with antibodies to human Bcl-X<sub>L</sub>, Bcl-2, Bax, Bak, Puma, Bim, Bmf, Bad, phospho-Bad, X-linked inhibitor of apoptosis protein (XIAP), and actin (Cell Signaling Technology, Danvers, MA), FADD (BD Transduction Labs, San Diego, CA), or caspase-8 (Immunotech, Fullerton, CA). DISC immune precipitation was performed as previously described.<sup>22</sup>

### Subcutaneous xenograft studies

The studies were conducted in compliance with National Institutes of Health Guide for the Care and Use of Laboratory Animals<sup>51</sup> and were approved by the Institutional Animal Care and Use Committee (IACUC) at Genentech. Female CB17 ICR SCID mice (Charles River Laboratories, Hollister, CA) were maintained in accordance with the Guide for the Care and Use of Laboratory Animals.<sup>51</sup> Ramos RA1 (5 × 10<sup>6</sup>), Ramos T1 (5 × 10<sup>6</sup>), BJAB (5 × 10<sup>6</sup>), SC-1 (10 × 10<sup>6</sup>), and DoHH-2 (20 × 10<sup>6</sup>) cells were harvested, suspended in PBS, and injected subcutaneously into the right dorsal flank of 6- to 8-week-old mice. When tumors reached 100 to 200 mm<sup>3</sup>, animals were randomized into groups, and dosed intraperitoneally with vehicle (0.5 M Arg-succinate/20 mM Tris/0.02% Tween 20, pH 7.2), 60 mg/kg Apo2L/TRAIL, and/or 4 mg/kg or 10 mg/kg rituximab (as noted in figure legends). Treatment schedule for rhApo2L/TRAIL was once a day for 5 days, 2 days off, followed by once a day for 5 days. Treatment

schedule for rituximab (at all dose levels) was once a week for 2 weeks. Tumor volumes were determined by measuring the length (l) and width (w) and calculating the volume using the following formula:  $V = lw^2/2$ .

**Studies with disseminated xenografts**

Female CB17 ICR SCID mice (Charles River Laboratories) were injected intravenously with  $5 \times 10^6$  BJAB-Luc cells. The mice were imaged weekly using the following procedure to monitor disease progression. Before image acquisition, the tumor-bearing mice were anesthetized using isoflurane and injected intraperitoneally with 200 mg/kg D-luciferin (Invitrogen, Carlsbad, CA). During image acquisition the mice were maintained on isoflurane by nose cone and body temperature was regulated using a warming pad. Bioluminescence images were acquired using a custom-designed cooled intensified charge-coupled device camera system. Image acquisition times varied according to signal intensity but were typically started at 6 seconds and decreased with tumor progression. Tumors were localized by overlaying a reference image of the mouse with the bioluminescence data image. Images were quantified using Image J version 1.37 (developed at the National Institutes of Health, Bethesda, MD, and available at <http://rsb.info.nih.gov/ij/>) by evaluating pixel intensities in the bioluminescence data image, applying an appropriate background correction, and scaling the resulting values to account for variations in acquisition time and camera settings to give a mean intensity in relative light units (RLU) that was representative of total disease burden. This approach has been validated by pathology and magnetic resonance imaging (MRI) (data not shown) for other comparable models. Tumor burden as assessed by total luminescence was monitored weekly. At day 13, mice were randomized into 4 groups with equivalent luminescence at which time treatment began. Mice were treated as described for subcutaneous tumors. At day 26, the difference in mean RLU between groups was analyzed using a nonparametric Mann-Whitney test.

Additional methods are in Document S1, available on the *Blood* website; see the Supplemental Materials link at the top of the online article.

**Results**

To evaluate the activity of rhApo2L/TRAIL against NHL and the ability of this ligand to cooperate with rituximab, we characterized a panel of NHL cell lines by flow cytometry for surface expression of the proapoptotic Apo2L/TRAIL receptors DR4 and DR5 and the decoy receptors DcR1 and DcR2, as well as for expression of the rituximab antigen CD20. All of the 7 cell lines examined expressed significant levels of DR4 and/or DR5 and had relatively low or undetectable levels of DcR1 and DcR2, as did the rituximab-resistant Ramos T1 variant (Figure 1A; Figure S1). Most of the cell lines, including Ramos T1, also expressed abundant CD20 levels, except OCI-Ly19 cells, which displayed very low CD20 expression (Figure 1B).

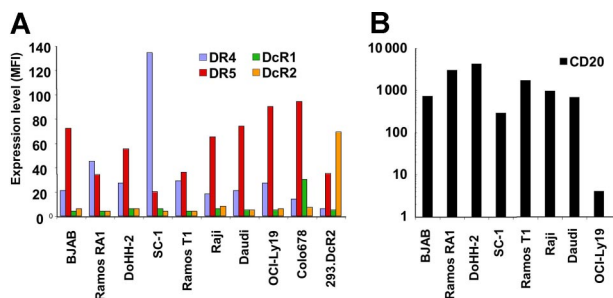


**Figure 1. Expression of Apo2L/TRAIL receptors and CD20 on cell lines.** A panel of NHL cell lines and 2 control cell lines were stained with PE-conjugated antibodies to DR4, DR5, DcR1, and DcR2 (A) and CD20 (B). Data are reported as mean fluorescence intensity (MFI). The background fluorescence for the isotype control antibody on all cell lines was an MFI less than 6.

**Table 1. Analysis of NHL cell lines for sensitivity to rhApo2L/TRAIL alone and in combination with rituximab**

Cell lines	NHL type	IC <sub>50</sub> , ng/mL	
		rhApo2L/TRAIL	rhApo2L/TRAIL + rituximab
BJAB	BL	32	26
Ramos RA1	BL	38	17
DoHH-2	FL	14	—*
SC-1	FL	> 1000	> 1000
Ramos T1	BL	33	13
Raji	BL	> 1000	> 1000
Daudi	BL	> 1000	> 1000
OCI-Ly19	DLBCL	> 1000	> 1000

BL indicates Burkitt lymphoma.

\*Rituximab (1000 ng/mL) has single-agent activity, which precludes comparing the IC<sub>50</sub> values of the cell viability curves for this cell line.

Next, we tested these cell lines in vitro for sensitivity to cell-death induction by rhApo2L/TRAIL (Table 1; Figure 2). Four of the cell lines (BJAB, Ramos RA1, Ramos T1, and DoHH-2) underwent cell death in response to rhApo2L/TRAIL, while the other 4 (SC-1, Raji, Daudi, and OCI-Ly19) did not. Rituximab showed no cytotoxic activity against BJAB, Ramos RA1, or SC-1 cells, but displayed some cytotoxicity against DoHH-2 cells (Figure 2A-D). Rituximab augmented the amount of cell death

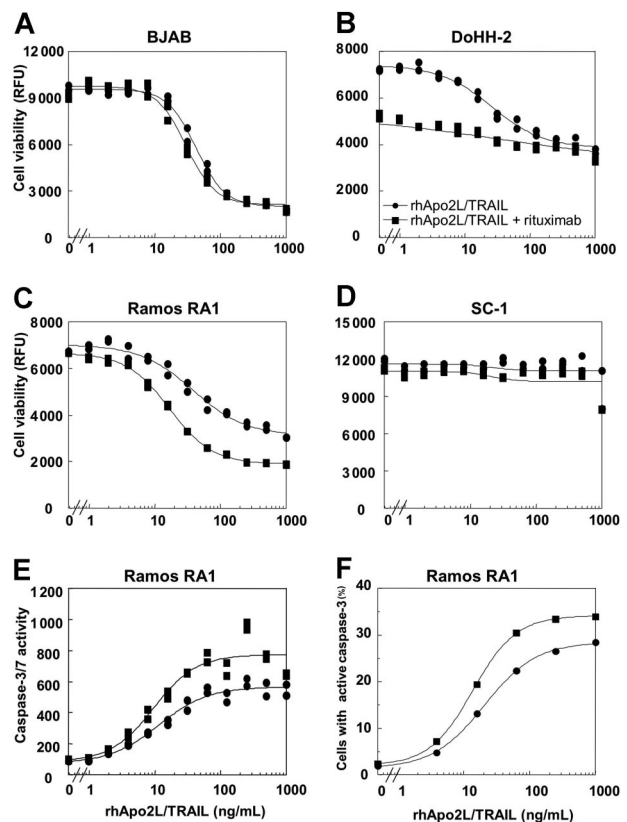


**Figure 2. rhApo2L/TRAIL induces apoptosis and caspase-3/7 activation in NHL cells.** BJAB (A), DoHH-2 (B), Ramos RA1 (C), and SC-1 (D) NHL cells were analyzed for cell viability by AlamarBlue staining after 48 hours of treatment with rhApo2L/TRAIL alone (●) or rhApo2L/TRAIL and rituximab (20 μg/mL, ■). Caspase-3/7 activity in Ramos RA1 cells was measured using a fluorescence assay after 24 hours of treatment under the conditions described for panels A-D. (E) Flow cytometric analyses of active caspase-3–positive Ramos RA1 cells as detected by a FITC-conjugated monoclonal antibody to active caspase-3 after 24 hours of treatment as described for panels A-D. (F) In every experiment, rhApo2L/TRAIL and rituximab were added simultaneously.

induced by rhApo2L/TRAIL in Ramos RA1 and DoHH-2 cells, but not in BJAB or SC-1 cells. Further analysis of Ramos RA1 cells indicated dose-dependent activation of caspase-3/7 upon treatment with rhApo2L/TRAIL (Figure 2E,F), confirming the induction of apoptosis. Rituximab by itself did not stimulate caspase-3/7 activity; however, it augmented rhApo2L/TRAIL-induced caspase-3/7 activation (Figure 2E). Flow cytometric analysis of caspase-3 activation at the individual cell level confirmed that rituximab did not directly stimulate caspase-3 and indicated that the number of cells with active caspase-3 increased when rituximab and rhApo2L/TRAIL were used together compared with rhApo2L/TRAIL alone (Figure 2F). Furthermore, pretreatment with rituximab did not change the percentage of cells with active caspase-3 at 24 hours compared with simultaneous treatment, but it did accelerate the rate of caspase-3 cleavage in those cells undergoing apoptosis (Figure S2). Together, these results demonstrated that 3 of 7 NHL cell lines tested were sensitive to rhApo2L/TRAIL, and of those, 2 showed evidence of enhancement by rituximab.

Follicular lymphomas overexpress Bcl-2 due to a characteristic chromosomal translocation t(14;18) that places the Bcl-2 protein coding region under the control of the IgH promoter/enhancer.<sup>52,53</sup> Expression of Bcl-2 can render FL cells more resistant to apoptotic stimuli.<sup>54</sup> To ascertain if resistance to rhApo2L/TRAIL correlated with Bcl-2 expression, we tested the panel of NHL cells for Bcl-2 expression by intracellular flow cytometry using a Bcl-2-specific antibody (Figure 3A). We also tested for the expression of Bcl-2 by immunoblot analysis (Figure 3B). Whereas the Burkitt lymphoma lines had low or undetectable amounts of Bcl-2, the FL cell lines DoHH-2 and SC-1 and the DLBCL line OCI-Ly19 expressed high Bcl-2 levels. Thus, there was no clear correlation between Bcl-2 expression and resistance to rhApo2L/TRAIL among the 8 cell lines tested.

To gain some mechanistic insight into how rituximab might augment rhApo2L/TRAIL-induced effector caspase activation, we examined whether this antibody affects proximal signaling events initiated by rhApo2L/TRAIL in Ramos RA1 cells. We observed no detectable change in cell surface levels of DR4 and DR5 after a 24-hour exposure to 20  $\mu\text{g}/\text{mL}$  rituximab (Figure S3A). Rituximab also did not substantially alter the recruitment of FADD and caspase-8 to the rhApo2L/TRAIL DISC (Figure S3B), suggesting that the antibody may modulate events distal to the DISC to augment effector caspase activation. To assess this further, we analyzed Ramos RA1 cells for changes in the levels of the antiapoptotic Bcl-2 homolog Bcl-X<sub>L</sub>; the proapoptotic BH3-only proteins Bax, Bak, Bad, Puma, Bim, Bmf, Bad, and phospho-Bad; and the inhibitor of apoptosis protein XIAP, by immunoblot (Figure 3C). We observed no major changes in any of the proapoptotic or antiapoptotic proteins tested. To examine the possibility that other proapoptotic modulators not included in our analysis might be altered by rituximab treatment, we generated a Ramos RA1 cell line overexpressing Bcl-2, which inhibits multiple BH3-only Bcl-2 family member proteins.<sup>55</sup> We confirmed expression of high Bcl-2 levels by immunoblot analysis (Figure S3D). Bcl-2 overexpression diminished the activation of caspase-3 by rhApo2L/TRAIL alone (Figure 3C,D), consistent with a type II cell phenotype. Importantly, Bcl-2 overexpression also attenuated the ability of rituximab to augment caspase-3 activation. Moreover, Bcl-2 overexpression inhibited rituximab augmentation of rhApo2L/TRAIL-induced mitochondrial permeability transition 24 hours after treatment (Figure 3E,F). Thus, experimental overexpres-

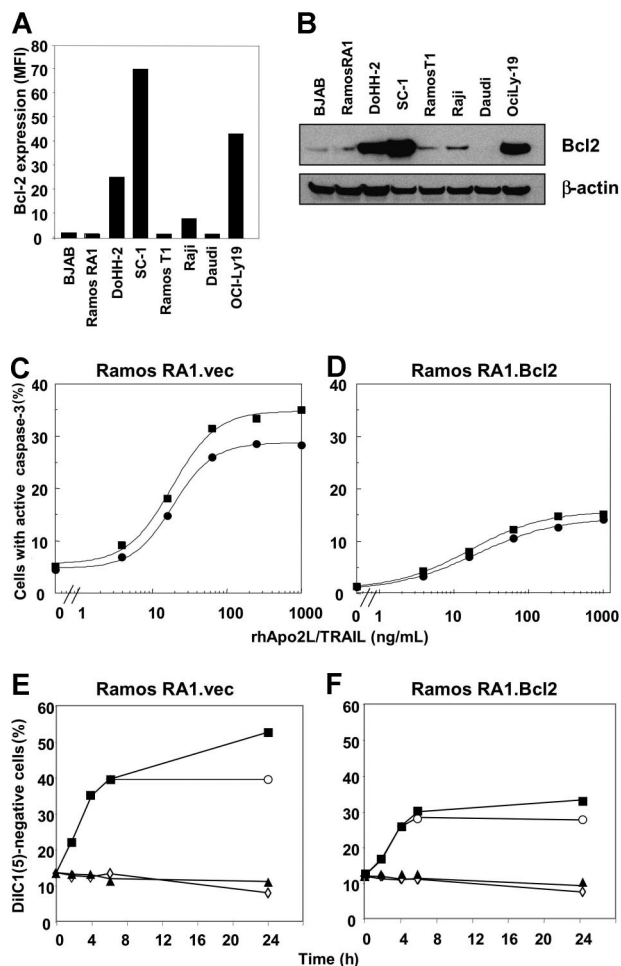
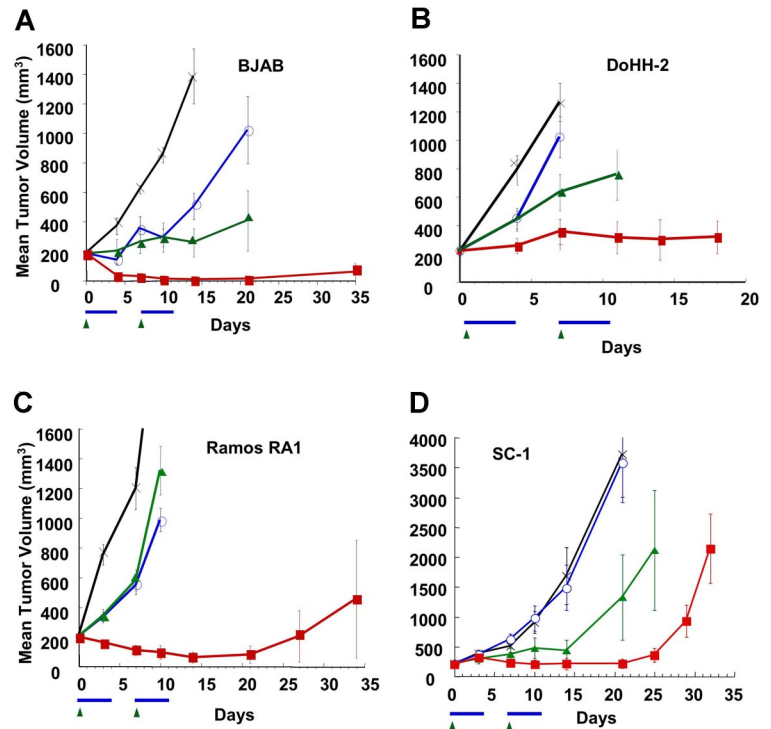


**Figure 3. Modulation of proapoptotic and antiapoptotic Bcl-2 family proteins by rituximab in Ramos RA1 cells.** (A) Flow cytometric analysis of Bcl-2 levels in NHL cell lines. Data are reported as MFI. The background fluorescence for the isotype control antibody on all cell lines was an MFI less than 6. (B) Immunoblot analysis of Bcl-2 expression in NHL cell lines. (C,D) Effect of Bcl-2 overexpression in Ramos RA1 cells on caspase-3 activation. Flow cytometric analyses of active caspase-3-positive Ramos RA1 cells treated with rhApo2L/TRAIL alone ( $\bullet$ ) or rhApo2L/TRAIL and rituximab (20  $\mu\text{g}/\text{mL}$ ,  $\blacksquare$ ) for 24 hours. (E,F) Effect of Bcl-2 overexpression in Ramos RA1 cells on loss of mitochondrial-membrane integrity. Flow cytometric analyses of DiIC<sub>1</sub>(5)-negative Ramos RA1 cells treated with vehicle ( $\diamond$ ), rhApo2L/TRAIL (1  $\mu\text{g}/\text{mL}$ ,  $\circ$ ), rituximab (20  $\mu\text{g}/\text{mL}$ ,  $\blacktriangle$ ), or rhApo2L/TRAIL and rituximab ( $\blacksquare$ ). Cells were analyzed for DiIC<sub>1</sub>(5) at the indicated number of hours after addition of rhApo2L/TRAIL.

sion of Bcl-2 in Ramos RA1 cells reduces the augmentation of rhApo2L/TRAIL-induced apoptosis by rituximab.

To test the activity of rhApo2L/TRAIL in vivo, we established xenograft models based on several human NHL cell lines in SCID mice. We implanted NHL cells under the skin and allowed subcutaneous tumors to develop to a size of approximately 200 mm<sup>3</sup> before beginning therapy. Treatment of mice harboring BJAB tumors with rhApo2L/TRAIL or rituximab caused a clear delay in tumor growth; however, none of the tumors showed partial or complete regression (defined as at least 50% or 100% shrinkage, respectively; Figure 4A; Table 2). In contrast, combined treatment with rhApo2L/TRAIL plus rituximab led to a much more prolonged delay in tumor growth, with 1/7 and 6/7 tumors, respectively, showing partial or complete regression. In mice bearing DoHH-2 xenografts, rhApo2L/TRAIL treatment caused a minimal effect, while rituximab therapy led to a more substantial tumor-growth delay but not

**Figure 4. Activity of rhApo2L/TRAIL and rituximab against subcutaneous NHL xenografts.** CB17 ICR SCID mice bearing established B220 (A; n = 7 mice/group), DoHH-2 (B; n = 10 mice/group), Ramos RA1 (C; n = 9 mice/group), and SC-1 (D; n = 6 mice/group) tumors (approximately 200 mm<sup>3</sup> in size) were treated with vehicle (black x), 60 mg/kg rhApo2L/TRAIL (open blue circle), 4 mg/kg rituximab (closed green triangle), or rhApo2L/TRAIL and rituximab (closed red square). rhApo2L/TRAIL was administered daily for 5 consecutive days followed by a 2-day break and a second 5-day treatment as indicated by the blue bar. Rituximab was administered once a week as indicated by the green arrow.



tumor regression (Figure 4B; Table 2). The combination of rhApo2L/TRAIL with rituximab was significantly more effective at abating tumor progression, with 1/7 tumors showing partial shrinkage and 1/7 having complete regression. Monotherapy of mice bearing Ramos RA1 xenografts with rhApo2L/TRAIL or rituximab resulted in a minor delay of tumor growth with no partial or complete responses (Figure 4C; Table 2). Again, combined therapy with rhApo2L/TRAIL and rituximab

led to a substantially greater delay in tumor growth, with 2/9 (22%) or 7/9 (78%) tumors showing partial or complete regression. Treatment of mice harboring SC-1 xenografts with rhApo2L/TRAIL alone had no measurable effect, while rituximab treatment delayed tumor growth (Figure 4D; Table 2). Combined treatment with rhApo2L/TRAIL plus rituximab caused further growth delay, with 1/6 (17%) partial and 2/6 (33%) complete tumor regressions. In contrast to the latter models, treatment of mice carrying Raji xenografts with rhApo2L/TRAIL did not inhibit tumor growth, and while rituximab modestly slowed tumor growth, the combination showed no added benefit (Figure S4). Likewise, treatment of mice carrying OCI-Ly19 xenografts with rhApo2L/TRAIL or rituximab or both did not inhibit tumor growth (data not shown). These results indicate that rhApo2L/TRAIL and rituximab can cooperate to attenuate or reverse growth of several NHL-based tumor xenografts. This *in vivo* cooperation applies to cell lines that are sensitive *in vitro* to cytotoxicity of one or both agents, as well as to some, though not to all, of the cell lines that are resistant to both.

**Table 2. Activity of rhApo2L/TRAIL and rituximab against NHL xenografts**

Cell line/treatment	PR	CR
<b>B220</b>		
Vehicle	0/7	0/7
rhApo2L/TRAIL	2/7	0/7
Rituximab	2/7	0/7
Combination	1/7	6/7
<b>Ramos RA1</b>		
Vehicle	0/9	0/9
rhApo2L/TRAIL	0/9	0/9
Rituximab	0/9	0/9
Combination	1/9	7/9
<b>DoHH-2</b>		
Vehicle	0/10	0/10
rhApo2L/TRAIL	0/10	0/10
Rituximab	0/10	0/10
Combination	1/10	1/10
<b>SC-1</b>		
Vehicle	0/6	0/6
rhApo2L/TRAIL	0/6	0/6
Rituximab	1/6	2/6
Combination	1/6	2/6

CB17 ICR SCID mice bearing established NHL tumors (approximately 200 mm<sup>3</sup> in size) were treated with indicated therapeutic. A partial response (PR) is defined as at least 50% tumor shrinkage and a complete response (CR) as 100% shrinkage. rhApo2L/TRAIL was administered daily for 5 consecutive days followed by a 2-day break. Rituximab was administered once a week. Both therapeutics were administered for 2 weeks. Data are number responding/number in treatment group.

Rituximab exerts antitumor activity *in vivo* through several mechanisms, including antibody-dependent cell-mediated cytotoxicity (ADCC) and complement-dependent cytotoxicity (CDC). We investigated the ability of rhApo2L/TRAIL to cooperate with rituximab in an NK-dependent ADCC assay *in vitro* (Figure S5A). We observed a modest enhancement of rituximab mediated ADCC in the presence of rhApo2L/TRAIL; whereas, rhApo2L/TRAIL alone showed no ADCC activity. To investigate whether these activities are important for rituximab's cooperation with rhApo2L/TRAIL *in vivo*, we used previously established pharmacologic approaches to inhibit specific antibody-mediated effector functions and examined the impact on anti-tumor activity in mice bearing Ramos RA1 tumor xenografts (Figure 5). We depleted NK cells, which can support ADCC by virtue of Fcγ receptor expression, in mice bearing

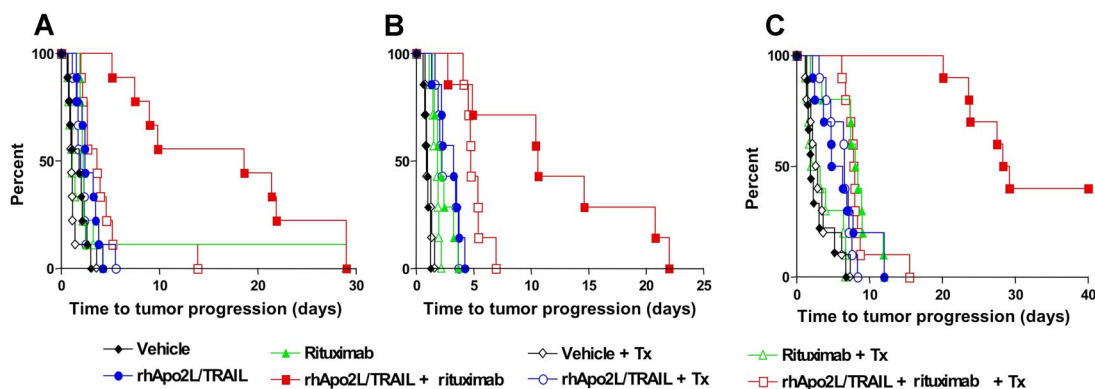


**Figure 5.** Effect of NK cell depletion and complement depletion on cooperation between rituximab and rhApo2L/TRAIL against Ramos RA1 xenografts. CB17 ICR SCID mice bearing subcutaneous Ramos RA1 xenografts were treated (Tx) with rabbit anti-asialo GM1 antibody (aGM1) to deplete NK cells (A;  $n = 9$  mice/group), cobra venom factor (CVF) to deplete complement protein C3 (B;  $n = 7$  mice/group), or aGM1 and CVF (C;  $n = 10$  mice/group) one day prior to the initiation of treatment with vehicle (V), 60 mg/kg rhApo2L/TRAIL (A), 4 mg/kg rituximab (R), or rhApo2L/TRAIL and rituximab (A + R). The data are graphed as a Kaplan-Meier analysis of the time for the tumors to reach 2.5 times their starting size. The aGM1 antibody and CVF were administered 2 times per week for the duration of the experiment. rhApo2L/TRAIL was administered daily for 5 consecutive days followed by a 2-day break and a second round of 5 days of treatment. Rituximab was administered once a week for 2 weeks.

Ramos RA1 tumors with anti-asialo GM1 antibodies before the start of therapy. NK cell depletion was confirmed by analyzing the spleen for NK cells (CD49b<sup>+</sup>) by flow cytometry (Figure S5B). Consistent with the other Ramos RA1 data (Figure 4B), combined treatment with rituximab and rhApo2L/TRAIL lead to a significant tumor-growth delay (Figure 5A). NK cell depletion did not affect the rate of tumor growth (depicted as a Kaplan-Meier analysis of the time interval for the tumors to reach 2.5-fold their starting volume) in mice treated with vehicle, rhApo2L/TRAIL, or rituximab; however, it substantially reduced therapeutic benefit in mice treated with rituximab plus rhApo2L/TRAIL compared with nondepleted controls ( $P = .001$  by log-rank test, Figure 5A).

Complement activation by immunoglobulin is dependent on C3. Cobra venom factor (CVF) is a C3 convertase that catalyzes the complete degradation of all circulating C3 protein when administered to mice, preventing complement activation and target-cell killing. To block CDC, we treated Ramos RA1 tumor-bearing mice with CVF one day before commencing treatment with rhApo2L/TRAIL and/or rituximab and every 3 days thereafter (Figure 5B). Immunoblot analysis confirmed essentially complete depletion of serum C3 in CVF-treated animals for the duration of the study (Figure S5C). C3 depletion did not alter the rate of tumor growth in mice treated with vehicle, rhApo2L/TRAIL, or rituximab; however, it substantially prevented therapeutic benefit in mice treated with rituximab plus rhApo2L/TRAIL compared with nondepleted controls ( $P = .016$  by log-rank test, Figure 5B). Last, we simultaneously depleted both NK cells and complement to determine the impact on the efficacy of rhApo2L/TRAIL and rituximab (Figure 5C). As with elimination of either effector alone, elimination of both resulted in a significant loss of the combined activity of rhApo2L/TRAIL and rituximab ( $P = .02$  by log-rank test, Figure 5C). Taken together, these results suggest that both NK- and C3-dependent antibody-mediated mechanisms are important for the cooperation between rituximab and rhApo2L/TRAIL against Ramos RA1 xenografts.

Advanced NHL typically occurs as a disseminated malignancy. To examine the activity of rhApo2L/TRAIL against disseminated NHL tumors, we developed a model based on BJAB cells stably transfected with firefly luciferase (BJAB-Luc cells), which can be detected in vivo by luminescence after injection of a synthetic luciferase substrate. Within approximately 2 weeks after intravenous injection of BJAB-Luc cells

into SCID mice, detectable tumors were established in various tissue sites including lymph nodes and bone (Figure 6C and data not shown). We distributed mice with established 13-day-old BJAB-Luc tumors into treatment groups with an equivalent tumor burden as assessed by total luminescence (Figure 6A; Figure S6). After 2 weeks of treatment, mice that received vehicle showed a pronounced increase in tumor burden (compare vehicle group in Figure 6B,C; Figure S6). The BJAB-Luc tumors continued to grow in the presence of vehicle; rituximab alone did not appreciably inhibit tumor growth; however, mice treated with rhApo2L/TRAIL alone or in combination with rituximab showed significantly less tumor growth, with evidence of tumor regression or stasis in some animals. Mice treated with rituximab alone had 74% lower tumor burden compared with vehicle-treated mice ( $P = .062$ , Mann-Whitney test). Mice treated with rhApo2L/TRAIL alone had 84% less tumor burden ( $P = .009$  compared with vehicle, Mann-Whitney test). Mice treated with rhApo2L/TRAIL and rituximab had a 94% lower tumor burden than vehicle controls ( $P = .004$  compared with vehicle control,  $P = .057$  compared with rituximab alone and  $P = .275$  compared with rhApo2L/TRAIL alone, Mann-Whitney test). We also assessed tumor-associated morbidity (Figure 6D). Mice treated with rituximab or rhApo2L/TRAIL or both showed significant increases in survival compared with vehicle-treated controls ( $P = .015$ ,  $P = .045$ , or  $P = .001$ , respectively, by log-rank test). Importantly, while all animals in the monotherapy groups eventually succumbed to their tumor burden, 3 (30%) of 10 mice receiving rhApo2L/TRAIL plus rituximab survived more than 135 days, suggesting that these animals underwent complete tumor remission. These results indicate that both rhApo2L/TRAIL and rituximab exert significant antitumor activity against disseminated BJAB tumors, and the 2 agents can cooperate to attenuate, and in some cases even to eradicate, these tumors, increasing host survival.

Some NHL tumors can acquire resistance to rituximab in the clinical setting. In an effort to model rituximab resistance, we generated a rituximab-refractory Ramos RA1 cell line (Ramos T1) through multiple rounds of in vivo exposure to rituximab. Monotherapy of mice bearing subcutaneous Ramos T1 tumors with 4 or 10 mg/kg rituximab or with rhApo2L/TRAIL only slightly delayed tumor growth (Figure 7). However, combined treatment with rhApo2L/TRAIL plus either one of the rituximab doses led to a significant delay in tumor growth. At the 4-mg/kg rituximab

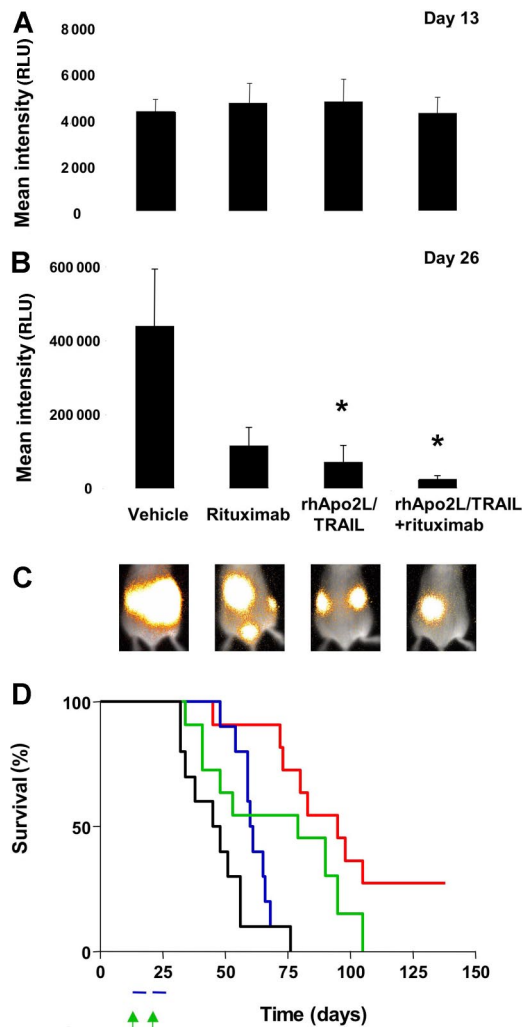


**Figure 6. Activity of rhApo2L/TRAIL and rituximab against disseminated NHL tumor xenografts.** BJAB-Luc cells were injected intravenously into CB17 ICR SCID mice. Tumor burden was determined by bioluminescent imaging and shown as the mean relative light units (RLU) for 4 randomized groups ( $n = 10$  mice/group) with equivalent tumor burden at day 13 (A). Mice were treated with vehicle, 60 mg/kg rhApo2L/TRAIL, 4 mg/kg rituximab, or rhApo2L/TRAIL and rituximab. rhApo2L/TRAIL was administered daily for 5 consecutive days followed by a 2-day break and a second round of 5 days of treatment as indicated by the blue bar (panel D). Rituximab was administered once a week for 2 weeks as indicated by the green arrow (panel D). On day 26 (B), the tumor burden for the rituximab group was marginally reduced ( $P = .062$  compared with vehicle, Mann-Whitney test), the tumor burden for the rhApo2L/TRAIL group was significantly lower ( $P = .009$  compared with vehicle), and the tumor burden of the rhApo2L/TRAIL and rituximab group was significantly lower than the vehicle control ( $P = .004$ ). The tumor burden for the rhApo2L/TRAIL and rituximab group was not significantly lower than the rhApo2L/TRAIL group ( $P = .275$ ); however, the tumor burden for the rhApo2L/TRAIL and rituximab group was significantly lower than the rituximab group ( $P = .057$ ). \* represents statistical significance of result compared to vehicle. Error bars in panels A and B represent SEM. (C) Representative false color images of the mean tumor luminescence for each group are shown as an overlay of the reference image of the whole mouse. (D) Survival analysis of the BJAB-bearing mice; Kaplan-Meier curves for the experiment are shown. The vehicle-treated (black line), rhApo2L/TRAIL-treated (blue line), rituximab-treated (green line), and rhApo2L/TRAIL and rituximab-treated (red line) mice are shown.

combination dose, 0 (0%) of 12 mice showed a partial response while 3 (25%) of 12 showed complete tumor regression. At the 10-mg/kg rituximab combination dose, 2 (17%) of 12 mice showed a partial response and another 6 (50%) of 12 showed complete tumor regression. These results suggest that addition of rhApo2L/TRAIL to rituximab may help overcome acquired rituximab resistance of certain NHL tumors.

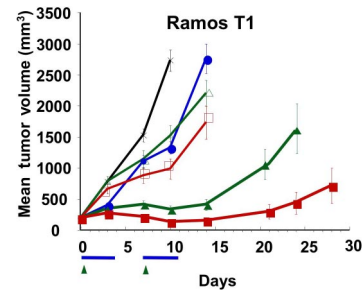


**Figure 7. Activity of rhApo2L/TRAIL and rituximab against a rituximab-refractory Ramos NHL variant.** A rituximab-refractory variant of Ramos RA1, designated Ramos T1, was established by treatment of Ramos RA1 in vivo with rituximab followed by harvest of tumors that escaped elimination and subsequent culture of cells. Ramos T1 cells were injected subcutaneously into CB17 ICR SCID mice and allowed to establish approximately 200-mm<sup>3</sup> tumors. Mice ( $n = 12$  mice/group) were then treated with vehicle (black x), 60 mg/kg rhApo2L/TRAIL (closed blue circle), 4 mg/kg rituximab (open green triangle), 10 mg/kg rituximab (open red square), rhApo2L/TRAIL and 4 mg/kg rituximab (closed green triangle), or rhApo2L/TRAIL and 10 mg/kg rituximab (closed red square). rhApo2L/TRAIL was administered daily for 5 consecutive days followed by a 2-day break and a second 5-day treatment as indicated by the blue bar. Rituximab was administered once a week as indicated by the green arrow.

## Discussion

It is now well established that members of the tumor necrosis factor superfamily have important roles in modulating the development and function of the immune system.<sup>56</sup> The role of Apo2L/TRAIL and its receptors in immunity has been the focus of several recent studies. Mice deficient in Apo2L/TRAIL or its sole murine proapoptotic receptor DR5 display essentially normal lymphoid development<sup>35,57</sup>; however, they show increased susceptibility to tumor initiation and metastasis.<sup>58,59</sup> Consistent with the possibility that Apo2L/TRAIL may be involved in antitumor immune functions, recombinant soluble Apo2L/TRAIL induces apoptosis in various types of cancer cells.<sup>38,60-62</sup> Several studies addressing specifically the sensitivity of hematologic malignancies to recombinant Apo2L/TRAIL in vitro show potent proapoptotic activity of the ligand,<sup>63-65</sup> often in combination with chemotherapeutic drugs, on Burkitt lymphoma cell lines.<sup>66-68</sup> Agonistic monoclonal antibodies to DR4 (TRAIL-R1) or DR5 (TRAIL-R2) have been shown to kill a limited subset of NHL cell lines and primary lymphoid tumors, mostly B-cell chronic lymphocytic leukemia (B-CLL)/small lymphocytic lymphoma (SLL).<sup>69</sup> However, none of these studies addresses the anti-NHL activity of rhApo2L/TRAIL in vivo, nor do they assess whether this proapoptotic receptor agonist can cooperate with other targeted agents such as rituximab.

In the present study, we investigated the activity of rhApo2L/TRAIL and its therapeutic interaction with rituximab in xenograft models of several NHL cell lines, including Burkitt, follicular, and diffuse large B-cell lymphomas. We observed proapoptotic activity of rhApo2L/TRAIL on 3 of 7 NHL cell lines in vitro. Consistent with earlier observations in other cancer cell types, the levels of DR4 or DR5 on these cells did not directly correlate with sensitivity to the ligand, suggesting the involvement of downstream mechanisms. Rituximab significantly augmented apoptosis induction by rhApo2L/TRAIL in Ramos RA1, and to a lesser extent, DoHH-2 cells, but not in BJAB or SC-1 cells. The enhancement in Ramos RA1 cell killing was associated with an increase in total caspase-3/7

activation as measured directly by enzymatic activity or indirectly by fluorescence-activated cell sorting (FACS) analysis with an antibody that specifically recognizes activated caspase-3. Rituximab did not alter apical signaling events induced by rhApo2L/TRAIL, suggesting that it may modulate more distal events that lead to activation of effector caspases. Consistent with this possibility, Bcl-2 overexpression attenuated rituximab's enhancement of rhApo2L/TRAIL-induced mitochondrial engagement and effector caspase activation. This observation is consistent with earlier evidence that rituximab can engage cell-intrinsic apoptotic changes even in the absence of effectors that could mediate ADCC and CDC.<sup>19</sup> It has been reported that Ramos RA1 cells undergo caspase-independent apoptosis upon treatment with cross-linked rituximab<sup>17</sup>; however, we did not observe evidence of cell death upon treatment of Ramos RA1 cells with non-cross-linked or cross-linked rituximab (Figure 2 and data not shown). Rituximab treatment of NHL cells also can sensitize to apoptosis activation by chemotherapeutic agents,<sup>70</sup> further suggesting that rituximab may affect the intrinsic apoptosis pathway.

Given the importance of antibody-mediated effector functions for rituximab's antitumor efficacy,<sup>11,15,16,71</sup> we extended our studies into *in vivo* NHL xenograft models. In keeping with our *in vitro* findings, rhApo2L/TRAIL and rituximab cooperated against Ramos RA1 and DoHH-2 xenografts. Notably, despite the absence of significant interaction against BJAB cells in culture, we observed a strong cooperation between rhApo2L/TRAIL and rituximab against BJAB xenografts *in vivo*. Moreover, while SC-1 cells were refractory to either one of the 2 agents *in vitro*, SC-1 tumor xenografts showed a significant response to rituximab monotherapy and a substantial further response to rituximab plus rhApo2L/TRAIL. Three of the lymphoma lines, BJAB, Ramos RA1, and DoHH-2, were highly responsive to rhApo2L/TRAIL *in vitro*; however, they showed minimal responses to rhApo2L/TRAIL alone *in vivo*. Perhaps the rapid clearance of rhApo2L/TRAIL in murine preclinical models contributes to this difference *in vivo*, as the half-life of rhApo2L/TRAIL in mice is approximately 3 to 5 minutes.<sup>72</sup> Certain lymphoma xenografts may require more sustained exposure to rhApo2L/TRAIL, therefore responding mainly in the setting of combination treatment with rituximab. Nonetheless, our results suggest that optimal cooperation between rhApo2L/TRAIL and rituximab is achieved *in vivo*, where both proapoptotic activity and antibody-mediated effector mechanisms may operate in conjunction. This conclusion is further supported by the observation that depletion of NK cells and complement substantially limited the therapeutic interaction between rituximab and rhApo2L/TRAIL *in vivo*.

Bcl-2 expression is a hallmark of FL and has been shown to attenuate sensitivity to apoptotic stimuli.<sup>54,73</sup> This could be a concern for therapeutic agents designed to target the apoptosis pathway. However, despite relatively high levels of Bcl-2 in the DoHH-2 and SC-1 FL cell lines, rhApo2L/TRAIL and rituximab cooperated effectively *in vivo* against tumor xenografts derived from these cell lines. Hence, it may be possible to overcome the tumor-protective effect of Bcl-2 by combining therapies that promote apoptosis together with nonapoptotic mechanisms such as ADCC and CDC.

The evidence that Fc gamma RIII polymorphism correlates with differential rituximab responsiveness in NHL patients strongly suggests that ADCC plays a key role in rituximab's efficacy.<sup>15,16</sup> Rituximab also has potent complement-fixing activity<sup>4</sup>; however,

there is conflicting data on the importance of this function for rituximab's efficacy in NHL patients.<sup>74,75</sup> Depletion of either NK cells or serum complement greatly attenuated the combined efficacy of rituximab and rhApo2L/TRAIL against Ramos RA1 xenografts. Thus, NK-mediated functions such as ADCC, as well as complement-mediated cytotoxicity, seem to contribute to the positive therapeutic interaction between the antibody and the ligand *in vivo*.

Because NHL progresses mainly as a systemic malignancy, we developed a model that allowed investigation of the activity of rhApo2L/TRAIL and rituximab against disseminated tumors. Within 2 weeks after intravenous injection, BJAB-Luc cells formed tumors in various tissue locations, including the lymph nodes and bone. While monotherapy with rituximab or rhApo2L/TRAIL was effective against systemic BJAB tumors, neither agent caused complete tumor regression. However, the combination of both therapies had greater efficacy, as suggested by prolonged survival and by an apparently complete tumor remission in 3 of 10 mice. It is intriguing that both rituximab and rhApo2L/TRAIL exerted stronger antitumor effects in the setting of disseminated compared with subcutaneous NHL tumor xenografts. This difference may be related to better drug accessibility of tumor cells in noncutaneous tissue sites. Alternatively, disseminated tumors may be more susceptible to the cytotoxic mechanisms exerted by these agents. Regardless, this observation is encouraging because disseminated tumors are likely to be better representative of the clinical situation than subcutaneous ones.

Some NHL patients become refractory to rituximab after an initial course of treatment. Of those patients who initially respond to rituximab and then relapse, only approximately 40% respond to a second course of treatment.<sup>76</sup> Loss of CD20 expression upon treatment is a rare event, suggesting that other mechanisms may underlie acquired rituximab resistance. We analyzed the expression of the anticomplement receptors CD55 and CD59 (Figure S7), but detected no differences in expression of the receptors between Ramos RA1 and Ramos T1 cells that might account for the resistance to rituximab. We generated a Ramos subline refractory to rituximab by repeated treatment of Ramos RA1 xenografts with the antibody. Like the majority of rituximab-relapsed human NHL tumors, the Ramos T1 line maintained expression of CD20. We assessed whether it might be possible to harness the positive therapeutic interaction between rhApo2L/TRAIL and rituximab to circumvent the acquired rituximab-resistance of this cell line. Upon reinjection into SCID mice, Ramos T1 tumors were relatively unresponsive to single-agent treatment with either rituximab or rhApo2L/TRAIL; however, these tumors showed substantially attenuated growth in response to treatment with the 2-drug combination, with up to 50% of tumors showing complete regression. These data suggest that the *in vivo* cooperation between rhApo2L/TRAIL and rituximab may help bypass treatment resistance of certain NHL tumors. Nonetheless, selection of patients for combination therapy based on biomarkers that may help predict response to rhApo2L/TRAIL would be expected to improve the response rate to combined rhApo2L/TRAIL and rituximab therapy. Recent work has identified specific markers that predict sensitivity to rhApo2L/TRAIL in epithelial cancers.<sup>77</sup> It will be important to investigate whether similar biomarkers may help guide patient selection in the NHL setting as well.

In conclusion, our studies provide the first evidence that the proapoptotic receptor agonist rhApo2L/TRAIL can exert activity *in vivo* against certain NHL xenografts. The antitumor



activity of rhApo2L/TRAIL was notably greater against disseminated compared with subcutaneous xenografts, suggesting better accessibility and/or greater sensitivity of dissipated tumors. We uncovered a remarkable *in vivo* cooperation between rhApo2L/TRAIL and rituximab—a targeted antibody that is approved by regulatory agencies and often used to treat certain types of NHL. The strong, positive therapeutic interaction between these 2 agents appears to arise from the integration of several tumor cell–killing mechanisms, including enhanced cell-autonomous apoptosis as well as antibody-mediated effector functions such as ADCC and CDC. The combination of rhApo2L/TRAIL with rituximab showed significant activity also against a rituximab-refractory Ramos tumor variant, suggesting that addition of rhApo2L/TRAIL to rituximab therapy may help overcome acquired resistance to rituximab. These findings provide a strong scientific rationale for clinical investigation of rhApo2L/TRAIL in combination with rituximab as a potential therapeutic strategy for NHL.

## References

- Clarke CA, Glaser SL. Changing incidence of non-Hodgkin lymphomas in the United States. *Cancer*. 2002;94:2015-2023.
- Armitage JO, Weisenburger DD. New approach to classifying non-Hodgkin's lymphomas: clinical features of the major histologic subtypes: Non-Hodgkin's Lymphoma Classification Project. *J Clin Oncol*. 1998;16:2780-2795.
- Taub R, Kirsch I, Morton C, et al. Translocation of the c-myc gene into the immunoglobulin heavy chain locus in human Burkitt lymphoma and murine plasmacytoma cells. *Proc Natl Acad Sci U S A*. 1982;79:7837-7841.
- Maloney DG, Grillo-Lopez AJ, White CA, et al. IDEC-C2B8 (Rituximab) anti-CD20 monoclonal antibody therapy in patients with relapsed low-grade non-Hodgkin's lymphoma. *Blood*. 1997;90:2188-2195.
- McLaughlin P, Grillo-Lopez AJ, Link BK, et al. Rituximab chimeric anti-CD20 monoclonal antibody therapy for relapsed indolent lymphoma: half of patients respond to a four-dose treatment program. *J Clin Oncol*. 1998;16:2825-2833.
- Piro LD, White CA, Grillo-Lopez AJ, et al. Extended Rituximab (anti-CD20 monoclonal antibody) therapy for relapsed or refractory low-grade or follicular non-Hodgkin's lymphoma. *Ann Oncol*. 1999;10:655-661.
- Davis TA, White CA, Grillo-Lopez AJ, et al. Single-agent monoclonal antibody efficacy in bulky non-Hodgkin's lymphoma: results of a phase II trial of rituximab. *J Clin Oncol*. 1999;17:1851-1857.
- Mounier N, Briere J, Gisselbrecht C, et al. Rituximab plus CHOP (R-CHOP) overcomes bcl-2-associated resistance to chemotherapy in elderly patients with diffuse large B-cell lymphoma (DLBCL). *Blood*. 2003;101:4279-4284.
- Riley JK, Sliwkowski MX. CD20: a gene in search of a function. *Semin Oncol*. 2000;27:17-24.
- Cragg MS, Walshe CA, Ivanov AO, Glennie MJ. The biology of CD20 and its potential as a target for mAb therapy. *Curr Dir Autoimmun*. 2005;8:140-174.
- Clynes RA, Towers TL, Presta LG, Ravetch JV. Inhibitory Fc receptors modulate *in vivo* cytotoxicity against tumor targets. *Nat Med*. 2000;6:443-446.
- Cragg MS, Glennie MJ. Antibody specificity controls *in vivo* effector mechanisms of anti-CD20 reagents. *Blood*. 2004;103:2738-2743.
- Wu J, Edberg JC, Redecha PB, et al. A novel polymorphism of FcγRIIIa (CD16) alters receptor function and predisposes to autoimmune disease. *J Clin Invest*. 1997;100:1059-1070.
- Shields RL, Namenuk AK, Hong K, et al. High resolution mapping of the binding site on human IgG1 for Fc gamma RI, Fc gamma RII, Fc gamma RIII, and FcRn and design of IgG1 variants with improved binding to the Fc gamma R. *J Biol Chem*. 2001;276:6591-6604.
- Cartron G, Dacheux L, Salles G, et al. Therapeutic activity of humanized anti-CD20 monoclonal antibody and polymorphism in IgG Fc receptor FcγRIIIa gene. *Blood*. 2002;99:754-758.
- Weng WK, Levy R. Two immunoglobulin G fragment C receptor polymorphisms independently predict response to rituximab in patients with follicular lymphoma. *J Clin Oncol*. 2003;21:3940-3947.
- van der Kolk LE, Evers LM, Omene C, et al. CD20-induced B cell death can bypass mitochondria and caspase activation. *Leukemia*. 2002;16:1735-1744.
- Demidem A, Lam T, Alas S, Hariharan K, Hanna N, Bonavida B. Chimeric anti-CD20 (IDEC-C2B8) monoclonal antibody sensitizes a B cell lymphoma cell line to cell killing by cytotoxic drugs. *Cancer Biother Radiopharm*. 1997;12:177-186.
- Jazirehi AR, Bonavida B. Cellular and molecular signal transduction pathways modulated by rituximab (rituxan, anti-CD20 mAb) in non-Hodgkin's lymphoma: implications in chemosensitization and therapeutic intervention. *Oncogene*. 2005;24:2121-2143.
- Ashkenazi A, Dixit VM. Death receptors: signaling and modulation. *Science*. 1998;281:1305-1308.
- Ashkenazi A. Targeting death and decoy receptors of the tumour-necrosis factor superfamily. *Nat Rev Cancer*. 2002;2:420-430.
- Kischkel FC, Lawrence DA, Chuntharapai A, Schow P, Kim KJ, Ashkenazi A. Apo2L/TRAIL-dependent recruitment of endogenous FADD and caspase-8 to death receptors 4 and 5. *Immunity*. 2000;12:611-620.
- Sprick MR, Weigand MA, Rieser E, et al. FADD/MORT1 and caspase-8 are recruited to TRAIL receptors 1 and 2 and are essential for apoptosis mediated by TRAIL receptor 2. *Immunity*. 2000;12:599-609.
- Kischkel FC, Lawrence DA, Tinel A, et al. Death receptor recruitment of endogenous caspase-10 and apoptosis initiation in the absence of caspase-8. *J Biol Chem*. 2001;276:46639-46646.
- Wang J, Chun HJ, Wong W, Spencer DM, Leonardo MJ. Caspase-10 is an initiator caspase in death receptor signaling. *Proc Natl Acad Sci U S A*. 2001;98:13884-13888.
- Sprick MR, Rieser E, Stahl H, Grosse-Wilde A, Weigand MA, Walczak H. Caspase-10 is recruited to and activated at the native TRAIL and CD95 death-inducing signalling complexes in a FADD-dependent manner but can not functionally substitute caspase-8. *EMBO J*. 2002;21:4520-4530.
- Kischkel FC, Hellbardt S, Behrmann I, et al. Cytotoxicity-dependent APO-1 (Fas/CD95)-associated proteins form a death-inducing signaling complex (DISC) with the receptor. *EMBO J*. 1995;14:5579-5588.
- LeBlanc HN, Ashkenazi A. Apo2L/TRAIL and its death and decoy receptors. *Cell Death Differ*. 2003;10:66-75.
- Peter ME, Krammer PH. The CD95(APO-1/Fas) DISC and beyond. *Cell Death Differ*. 2003;10:26-35.
- Li H, Zhu H, Xu CJ, Yuan J. Cleavage of BID by caspase 8 mediates the mitochondrial damage in the Fas pathway of apoptosis. *Cell*. 1998;94:491-501.
- Luo X, Budihardjo I, Zou H, Slaughter C, Wang X. Bid, a Bcl2 interacting protein, mediates cytochrome c release from mitochondria in response to activation of cell surface death receptors. *Cell*. 1998;94:481-490.
- Gross A, Yin XM, Wang K, et al. Caspase cleaved BID targets mitochondria and is required for cytochrome c release, while BCL-XL prevents this release but not tumor necrosis factor-R1/Fas death. *J Biol Chem*. 1999;274:1156-1163.
- Salvesen GS, Abrams JM. Caspase activation: stepping on the gas or releasing the brakes? lessons from humans and flies. *Oncogene*. 2004;23:2774-2784.
- Smyth MJ, Takeda K, Hayakawa Y, Peschon JJ, van den Brink MR, Yagita H. Nature's TRAIL: on a path to cancer immunotherapy. *Immunity*. 2003;18:1-6.
- Diehl GE, Yue HH, Hsieh K, et al. TRAIL-R as a negative regulator of innate immune cell responses. *Immunity*. 2004;21:877-889.
- Taieb J, Chaput N, Menard C, et al. A novel dendritic cell subset involved in tumor immunosurveillance. *Nat Med*. 2006;12:214-219.
- Mariani SM, Krammer PH. Differential regulation of TRAIL and CD95 ligand in transformed cells of the T and B lymphocyte lineage. *Eur J Immunol*. 1998;28:973-982.
- Ashkenazi A, Pai RC, Fong S, et al. Safety and antitumor activity of recombinant soluble Apo2 ligand. *J Clin Invest*. 1999;104:155-162.

## Acknowledgments

We thank Heather Maecker for technical advice on retroviral infections and Aaron Calestar for assistance on digital images.

## Authorship

Contribution: D.D. designed and performed the experiments and wrote the paper; B.Y., D.A.L., K.T., I.B., W.P.L., A.G., M.J.C., S.F.Y., and S.R. designed and performed the experiments; and A.A. designed the experiments and wrote the paper.

Conflict-of-interest disclosure: All the authors are employees of Genentech and declare competing financial interests.

Correspondence: Avi Ashkenazi, Department of Molecular Oncology, Genentech, Inc, 1 DNA Way, South San Francisco, CA 94080; e-mail: aa@gene.com.

39. Hymowitz SG, Christinger HW, Fuh G, et al. Triggering cell death: the crystal structure of Apo2L/TRAIL in a complex with death receptor 5. *Mol Cell*. 1999;4:563-571.
40. Hymowitz SG, O'Connell MP, Ultsch MH, et al. A unique zinc-binding site revealed by a high-resolution X-ray structure of homotrimeric Apo2L/TRAIL. *Biochemistry*. 2000;39:633-640.
41. Bodmer JL, Meier P, Tschopp J, Schneider P. Cysteine 230 is essential for the structure and activity of the cytotoxic ligand TRAIL. *J Biol Chem*. 2000;275:20632-20637.
42. Lawrence D, Shahroksh Z, Marsters S, et al. Differential hepatocyte toxicity of recombinant Apo2L/TRAIL versions. *Nat Med*. 2001;7:383-385.
43. Qin J, Chaturvedi V, Bonish B, Nickloff BJ. Avoiding premature apoptosis of normal epidermal cells. *Nat Med*. 2001;7:385-386.
44. Hao C, Song JH, Hsi B, et al. TRAIL inhibits tumor growth but is nontoxic to human hepatocytes in chimeric mice. *Cancer Res*. 2004;64:8502-8506.
45. Ganten TM, Koschny R, Sykora J, et al. Preclinical differentiation between apparently safe and potentially hepatotoxic applications of TRAIL either alone or in combination with chemotherapeutic drugs. *Clin Cancer Res*. 2006;12:2640-2646.
46. Kelley SK, Ashkenazi A. Targeting death receptors in cancer with Apo2L/TRAIL. *Curr Opin Pharmacol*. 2004;4:333-339.
47. Hylander BL, Pitoniak R, Penetrante RB, et al. The anti-tumor effect of Apo2L/TRAIL on patient pancreatic adenocarcinomas grown as xenografts in SCID mice. <http://www.translational-medicine.com/content/3/1/22>. Accessed October 22, 2007.
48. Baker BW, Boettiger D, Spooncer E, Norton JD. Efficient retroviral-mediated gene transfer into human B lymphoblastoid cells expressing mouse ecotropic viral receptor [letter]. *Nucleic Acids Res*. 1992;20:5234.
49. Pear WS, Nolan GP, Scott ML, Baltimore D. Production of high-titer helper-free retroviruses by transient transfection. *Proc Natl Acad Sci U S A*. 1993;90:8392-8396.
50. Belloc F, Belaud-Rotureau MA, Lavignolle V, et al. Flow cytometry detection of caspase 3 activation in preapoptotic leukemic cells. *Cytometry*. 2000;40:151-160.
51. National Research Council. Guide for the Care and Use of Laboratory Animals. Washington, DC: National Academy Press; 1985. NIH publication no. 86-23.
52. Yunis JJ, Oken MM, Kaplan ME, Ensrud KM, Howe RR, Theologides A. Distinctive chromosomal abnormalities in histologic subtypes of non-Hodgkin's lymphoma. *N Engl J Med*. 1982;307:1231-1236.
53. Tsujimoto Y, Cossman J, Jaffe E, Croce CM. Involvement of the bcl-2 gene in human follicular lymphoma. *Science*. 1985;228:1440-1443.
54. Johnson PW, Watt SM, Betts DR, et al. Isolated follicular lymphoma cells are resistant to apoptosis and can be grown in vitro in the CD40/stromal cell system. *Blood*. 1993;82:1848-1857.
55. Chen L, Willis SN, Wei A, et al. Differential targeting of prosurvival Bcl-2 proteins by their BH3-only ligands allows complementary apoptotic function. *Mol Cell*. 2005;17:393-403.
56. Locksley RM, Killeen N, Lenardo MJ. The TNF and TNF receptor superfamilies: integrating mammalian biology. *Cell*. 2001;104:487-501.
57. Finnberg N, Gruber JJ, Fei P, et al. DR5 knockout mice are compromised in radiation-induced apoptosis. *Mol Cell Biol*. 2005;25:2000-2013.
58. Sedger LM, Glaccum MB, Schuh JC, et al. Characterization of the in vivo function of TNF-alpha-related apoptosis-inducing ligand, TRAIL/Apo2L, using TRAIL/Apo2L gene-deficient mice. *Eur J Immunol*. 2002;32:2246-2254.
59. Cretney E, Takeda K, Yagita H, Glaccum M, Peshon JJ, Smyth MJ. Increased susceptibility to tumor initiation and metastasis in TNF-related apoptosis-inducing ligand-deficient mice. *J Immunol*. 2002;168:1356-1361.
60. Pitti RM, Marsters SA, Ruppert S, Donahue CJ, Moore A, Ashkenazi A. Induction of apoptosis by Apo-2 ligand, a new member of the tumor necrosis factor cytokine family. *J Biol Chem*. 1996;271:12687-12690.
61. Wiley SR, Schooley K, Smolak PJ, et al. Identification and characterization of a new member of the TNF family that induces apoptosis. *Immunity*. 1995;3:673-682.
62. Walczak H, Miller RE, Ariail K, et al. Tumoricidal activity of tumor necrosis factor-related apoptosis-inducing ligand in vivo. *Nat Med*. 1999;5:157-163.
63. Matsuda T, Almasan A, Tomita M, et al. Resistance to Apo2 ligand (Apo2L)/tumor necrosis factor-related apoptosis-inducing ligand (TRAIL)-mediated apoptosis and constitutive expression of Apo2L/TRAIL in human T-cell leukemia virus type 1-infected T-cell lines. *J Virol*. 2005;79:1367-1378.
64. An J, Sun Y, Fisher M, Rettig MB. Antitumor effects of bortezomib (PS-341) on primary effusion lymphomas. *Leukemia*. 2004;18:1699-1704.
65. Cillessen SA, Meijer CJ, Ossenkuppe GJ, et al. Human soluble TRAIL/Apo2L induces apoptosis in a subpopulation of chemotherapy refractory nodal diffuse large B-cell lymphomas, determined by a highly sensitive in vitro apoptosis assay. *Br J Haematol*. 2006;134:283-293.
66. Hussain A, Doucet JP, Gutierrez M, et al. Tumor necrosis factor-related apoptosis-inducing ligand (TRAIL) and Fas apoptosis in Burkitt's lymphomas with loss of multiple pro-apoptotic proteins. *Haematologica*. 2003;88:167-175.
67. Ucur E, Mattern J, Wenger T, et al. Induction of apoptosis in experimental human B cell lymphomas by conditional TRAIL-expressing T cells. *Br J Cancer*. 2003;89:2155-2162.
68. Mouzaki A, Packham G. Regulation of tumour necrosis factor-related apoptosis-inducing ligand (TRAIL)-induced apoptosis in Burkitt's lymphoma cell lines. *Br J Haematol*. 2003;122:61-69.
69. Georgakis GV, Li Y, Humphreys R, et al. Activity of selective fully human agonistic antibodies to the TRAIL death receptors TRAIL-R1 and TRAIL-R2 in primary and cultured lymphoma cells: induction of apoptosis and enhancement of doxorubicin- and bortezomib-induced cell death. *Br J Haematol*. 2005;130:501-510.
70. Alas S, Emmanouilides C, Bonavida B. Inhibition of interleukin 10 by rituximab results in down-regulation of bcl-2 and sensitization of B-cell non-Hodgkin's lymphoma to apoptosis. *Clin Cancer Res*. 2001;7:709-723.
71. Imai K, Takaoka A. Comparing antibody and small-molecule therapies for cancer. *Nat Rev Cancer*. 2006;6:714-727.
72. Kelley SK, Harris LA, Xie D, et al. Preclinical studies to predict the disposition of Apo2L/tumor necrosis factor-related apoptosis-inducing ligand in humans: characterization of in vivo efficacy, pharmacokinetics, and safety. *J Pharmacol Exp Ther*. 2001;299:31-38.
73. Jazirehi AR, Vega MI, Chatterjee D, Goodlick L, Bonavida B. Inhibition of the Raf-MEK1/2-ERK1/2 signaling pathway, Bcl-xL down-regulation, and chemosensitization of non-Hodgkin's lymphoma B cells by Rituximab. *Cancer Res*. 2004;64:7117-7126.
74. Weng WK, Levy R. Expression of complement inhibitors CD46, CD55, and CD59 on tumor cells does not predict clinical outcome after rituximab treatment in follicular non-Hodgkin lymphoma. *Blood*. 2001;98:1352-1357.
75. Treon SP, Mitsiades C, Mitsiades N, et al. Tumor cell expression of CD59 is associated with resistance to CD20 serotherapy in patients with B-cell malignancies. *J Immunother*. 2001;24:263-271.
76. Davis TA, Grillo-Lopez AJ, White CA, et al. Rituximab anti-CD20 monoclonal antibody therapy in non-Hodgkin's lymphoma: safety and efficacy of re-treatment. *J Clin Oncol*. 2000;18:3135-3143.
77. Wagner KW, Punnoose EA, Januario T, et al. Death receptor O-glycosylation controls tumor-cell sensitivity to the proapoptotic ligand Apo2L/TRAIL. *Nat Med*. 2007;13:1070-1077.